PROCESSING AND CHARACTERISATION OF LARGE AREA BURIED CONTACT SOLAR CELLS ON MULTICRYSTALLINE SILICON WITH A RECORD EFFICIENCY OF 17.5%

W. Jooss, B. Fischer, P. Fath,
S. Roberts*, T.M. Bruton*

University of Konstanz, Department of Physics, P.O.Box X916, D-78457 Konstanz, Germany
Phone: ++49-7531-88-2074,   Fax: ++49-7531-88-3895
Author for correspondence: Wolfgang Jooss, e-mail: Wolfgang.Jooss@uni-konstanz.de
*BP Solar, 12 Brooklands Close, Sunbury-on-Thames, Mddx TW16 7DX, United Kingdom

ABSTRACT: This paper describes the processing and characterisation of large area multicrystalline silicon solar cells using the buried contact solar cell technology. For the reduction of reflection losses, mechanical V-texturing is introduced into the processing sequence. Bulk passivation of crystal defects is carried out by remote plasma hydrogenation and an optimum process temperature of 450°C was determined for this process step. A record high efficiency for a large area multicrystalline silicon solar cell of 17.5% (V_{oc}=628 mV, J_{sc}=36.3 mA/cm^2, FF=76.8%, cell area 144 cm^2, independently confirmed at FhG-ISE, Germany) was obtained on Polix material. A loss analysis is carried out to determine the optical as well as recombination losses. Based on this analysis, the potential for a further increase in solar cell efficiency is discussed.
Keywords: Buried Contacts – 1: High-Efficiency – 2: Texturisation - 3

1 INTRODUCTION

Multicrystalline silicon (mc-Si) is a very attractive material for solar cell processing due to its lower wafer costs compared to monocrystalline Si. In the last years, the world wide production of crystalline silicon modules has shifted from mono-Si to mc-Si. However, the efficiency of mc-Si solar cells is currently lower than that of mono-Si, which is mainly caused by its intrinsic properties. The wafers have extended crystallographic defects like grain boundaries, dislocations and stacking faults, which are often inhomogeneously distributed. The concentration of lifetime killing metallic impurities can be high in these materials. The consequence of the defects is a lower lifetime of minority charge carriers in the as-cut wafer compared to their monocrystalline counterparts. However, the lifetime can be enhanced by hydrogen passivation of crystal defects and by gettering of metallic impurities during solar cell processing. With the optimisation of bulk passivation, diffusion lengths comparable to mono-Si can be achieved, therefore reducing the efficiency gap between mono-Si and mc-Si solar cells. Additionally, it can be expected, that the optimisation of the crystallisation process will enhance the material quality in the future. Therefore it is important to investigate solar cell designs and associated industrial process sequences, which take full benefit of a high quality mc-Si material with bulk diffusion lengths in the range of the cell thickness.

On small and medium cell sizes, efficiencies of 19.8% (cell area of 1 cm^2, [1]) and 18.3% (25 cm^2, [2]) have been reported on mc-Si solar cells. However, small solar cells do not take into account the spatial inhomogeneity of the mc-Si material. On larger substrate sizes, which are important for large-scale industrial production, an efficiency of 17.2% was demonstrated in [3] on a substrate size of 100 cm^2 and 17.1 cm^2 on 225 cm^2 [4]. In a recent publication [5], we have reported an efficiency of 17.5% on a cell area of 144 cm^2 using the Buried Contact Solar Cell (BCSC) design. This paper describes the processing and characterisation of the solar cell in more detail. The applied process includes mechanical V-texturing of the front surface for the
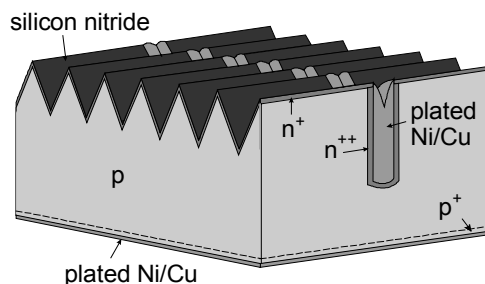

Figure 1: Schematic illustration of a mechanically V-textured BCSC with selective emitter. The front surface is coated by SiN$_x$ as single layer ARC, the contact grooves are perpendicular to the V-texture, the rear surface is passivated by an Al-BSF and metallisation is performed by electroless plating of Ni/Cu.

reduction of reflection losses and bulk passivation of crystal defects by remote hydrogen plasma treatments.

2 BURIED CONTACT SOLAR CELLS

The buried contact solar cell technology was invented and patented at the University of New South Wales in the late eighties [6]. This work was motivated by the fabrication of high efficiency solar cells applying low cost technologies. The device design of BCSCs includes features that are necessary to reach high conversion efficiencies: surface passivation on the front and rear side, a selective emitter structure and a high quality metallisation with low shadowing losses. The solar cells are metallised by introducing narrow grooves into the wafer by either laser scribing or mechanical abrasion. The width of the contact fingers is in the range of 20-30 µm which is significantly smaller than for screen printed solar cells. Despite the narrow contact fingers, an excellent finger conductivity is accomplished due to the depth of the grooves, which is in the range of 40-50 µm. The solar cell is generally metallised by the electroless deposition of Ni and Cu, which can be followed by the

deposition of a thin layer of Ag. First a thin layer of Ni is deposited that establishes the contact to the Si, whereas the current is transported in a thicker layer of Cu (several µm).

Currently BCSCs are produced by BP Solar in large scale industrial manufacturing using Cz-Si. BP Solar's current manufacturing capacity for SATURN BCSCs is 20 MWP. New production facilities are currently being installed leading to an annual output 50 MWp in 2003. Efficiencies in production range between 16 and 17%, but an efficiency of 18% was recently demonstrated in pilot-line production [7]. The objective of this work is to combine the advantages of the BCSC technology with the lower cost mc-Si material.

The investigated device design of this work is illustrated in Figure 1. For an effective reduction of front surface reflection losses, V-grooves are formed on the front side by mechanical abrasion. Additionally, the front side is covered by a single layer ARC of silicon nitride. The contact grooves are perpendicular to the V-grooves to reduce series resistance losses. The rear surface is passivated by an Al-BSF.

3 PROCESSING SEQUENCE

The sequence for the processing of mc-Si BCSCs is given in Figure 2. The process starts with mechanical V-texturing using an automatic dicing machine equipped with bevelled dicing blades or texturing wheels (see section 4) followed by saw damage removal. Emitter diffusion is carried out in an open-tube quartz furnace using a liquid $POCl_3$-source (emitter sheet resistance of 100-110 Ω/sqr). The phosphorous diffusion glass is removed in a diluted solution of HF prior to the deposition of silicon nitride in a Low Pressure CVD-reactor. SiN_x has to fulfil various requirements: it must act as a mask during the second heavy emitter diffusion and during wet chemical process steps such as groove etching and electroless plating. It additionally passivates the front surface and serves as an Antireflection Coating (ARC). The contact grooves are introduced by mechanical abrasion using 15 µm wide dicing blades. The saw damage within the grooves is removed in a hot solution of sodium hydroxide leading to a groove width of about 25 µm and a depth of about 40 µm (measured from the bottom of the V-grooves for textured solar cells). The contact grooves receive a deep emitter diffusion using a $POCl_3$ source at a temperature of 950 °C for 30 min ($R_{sheet} \approx 10$ Ω/sqr). In previous investigations [8], a thin layer of Al (2 µm) was deposited by electron beam evaporation to form the Al-BSF by alloying. Rear surface passivation by the thin Al-BSF is rather moderate. In this experiment, a thicker layer of Al is deposited by screen printing of Al paste. After firing in a belt furnace, the rear contact metal is removed in HCl exposing the doped p^+-region (Al-BSF). Hydrogen passivation of crystal defects is performed by remote plasma hydrogenation using a Microwave Induced Remote Hydrogen Plasma (MIRHP)- reactor (see section 5). The solar cells are metallised by electroless plating of Ni and Cu. After Ni-plating, the Ni is generally sintered to enhance the adhesion of the metallisation and to reduce the contact resistance. Due to the lack of suitable equipment, Ni-sintering can currently
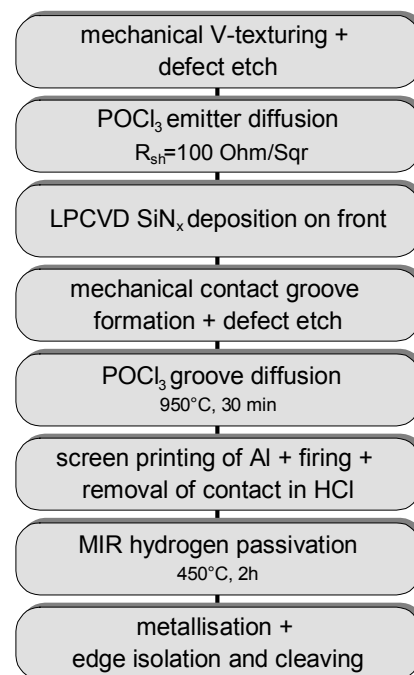

Figure 2: Process flow for the fabrication of mechanically V-textured buried contact solar cells including remote hydrogen plasma passivation in a MIRHP-reactor.

not be performed on substrate sizes exceeding 100 cm² at the University of Konstanz. To overcome this problem, a thin layer of Al was deposited on the rear by electron beam evaporation prior to Ni-plating, leading to an improved adhesion of the rear contact. The adhesion of the front contact was sufficient without sintering. Al-evaporation will be omitted in future experiments once a furnace for Ni-sintering is installed at UKN. Solar cell processing is completed by edge isolation using mechanical dicing and cleaving.

4 MECHANICAL V-TEXTURING

Front surface reflection is a considerable loss mechanism in crystalline silicon solar cells. In addition to an ARC, front surface reflectance can be further reduced by texturing the surface. The most commonly used texturisation method in industrial manufacturing is anisotropic alkaline texturing leading to random pyramids on <100> surfaces. However, alkaline texturing is not very effective for mc-Si due to the different crystal grain orientations. Effective techniques for surface texturing on mc-Si need to be independent of the crystal grain orientation. Several techniques have been investigated by several groups in recent years including acidic texturing, dry plasma etching using reactive gases and physical methods like mechanical texturing. In this work, we have applied mechanical V-texturing, which was intensively investigated at the University of Konstanz in recent years. In this approach, automatic dicing machines are equipped with either profiled texturing wheels or single bevelled dicing blades. The first technology is more appropriate for industrial manufacturing. The angle at the V-tips is between 60 and

100°, the depth of the V-texture is generally between 70 to 100 μm. Details on automatic texturing machines can be found in [9].

For a quantification of the reduction of front surface reflectivity, test structures were processed. Three different textures on mc-Si have been investigated: alkaline texturing, V-texturing with a structuring wheel (texturing angle 80°) and V-texturing with single blades (texturing angle 60°). For reference, alkaline textured Cz-Si samples were processed. Each wafer was additionally coated with an ARC of LPCVD SiN_x with a thickness of 75 nm (n≈2). From the test samples, the front surface reflectivity was measured and weighted with the solar spectrum (AM1.5) to determine the weighted reflectance. In Table I, the weighted reflectance and the optical losses in mA/cm² is given for the wavelength range from 300-1000 nm.

Table I: Optical characterisation of differently textured front surfaces on mc-Si and Cz-Si in the wavelength range from 300-1000 nm.

	Alk. mc	V-text. Wheel, mc	V-text. SB, mc-Si	Alk. Cz-Si
Optical loss [mA/cm²]	3.21	2.03	1.26	1.13
Weighted reflec. [%]	8.97	5.68	3.51	3.16

Mechanical V-texturing applying a texturing wheel reduces the optical losses by 1.2 mA/cm² compared to alkaline textured mc-Si. The losses are further reduced by 0.8 mA/cm² for single blade texturing, leading to about the same losses as random pyramids on Cz-Si. Concerning the optical differences between wheel and single blade texturing, the main difference is in a higher curvature radius in the bottom of the V-grooves for wheel-texturing. This leads to a higher front surface reflectivity.

Besides a reduction of front surface reflectivity, V-texturing leads to (1) an enhancement in collection probability of minority charge carriers and higher carrier generation in regions close to the emitter, and (2) improved light trapping [10].

V-texturing also enlarges the front surface area. The enlargement in surface area increases the contribution of the emitter to the first diode J_{01e} and also increases the saturation current density of the second diode J_{02}. The detrimental effect in the first case is not severe, since J_{01e} is low for BCSCs due to a good quality emitter and front surface passivation. However, J_{02} can be high for mc-Si solar cells (see section 5.2) and V-texturing can therefore reduce the fill factor and V_{oc}.

4 HYDROGEN PASSIVATION

It has been demonstrated in several investigations that the incorporation of hydrogen can reduce the recombination activity of various defects in mc-Si. Different techniques have been applied, including: forming gas anneals, silicon nitride layers containing hydrogen and hydrogen plasma processes. Currently, only hydrogen-rich PECVD SiN_x layers are used in large scale industrial production lines for hydrogenation. However, the application of PECVD SiN_x for
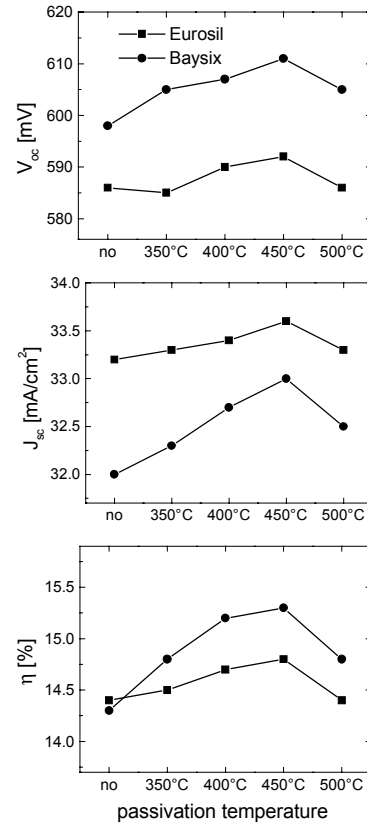

Figure 3: V_{oc}, J_{sc} and η of Baysix and Eurosil mc-Si BCSCs. The cells were subjected to remote hydrogen plasma passivation in a MIRHP-reactor at different process temperatures.

hydrogenation in the processing of mc-Si BCSCs is questionable. It was shown in [11] that overplating can occur if PECVD SiN_x is used as a masking dielectric, especially on V-textured solar cells. Also, processing of BCSCs requires further lengthy high temperature process steps after the deposition of the dielectric for contact groove diffusion and Al-alloying. At these temperatures, most of the hydrogen could be released from the wafer.

In this work hydrogenation was carried out by remote plasma hydrogen passivation using a Microwave Induced Remote Hydrogen Plasma (MIRHP)-reactor described in more detail in [12]. In this approach, a gas mixture (containing e.g. H_2 or NH_3) is inserted in a microwave cavity, where the gases are dissociated to generate atomic hydrogen. The samples are located in a quartz tube where a continuous gas flow is achieved by a pump at the exit. Since the front surface is coated by LPCVD SiN_x, which acts as diffusion barrier at the applied process temperatures, the hydrogen enters the wafer at the rear surface.

In a first experiment, the optimum process temperature for remote plasma hydrogen passivation was determined. The experiment was carried out on Baysix from Bayer (wafer thickness w=330 μm, ρ=1.0 Ωcm) and Eurosil from Eurosolare (w=350 μm, ρ=1.8 Ωcm). Processing was performed according to the sequence given in Figure 2 without mechanical V-texturing. The temperature was varied between 350 °C and 500 °C and the passivation time was 120 min. J_{sc}, V_{oc} and η are given

as a function of the process temperature for the two materials in Figure 3. It can be seen, that the optimum process temperature is 450 °C. At this temperature an improvement in efficiency of 1.0%abs. was reached on Baysix and of 0.4%abs. on Eurosil material.

5 HIGH EFFICIENCY SOLAR CELLS

Solar cell processing was carried out on Baysix (ρ=1.0 Ωcm, w=330 μm) and Polix from Photowatt (ρ=0.5 Ωcm, w=350 μm) on a wafer area of 12.5x12.5 cm^2. Processing started with mechanical V-texturing (single blades, texturing angle 60°) followed by saw damage removal. The remaining processing steps were carried out as indicated in Figure 2 with remote plasma hydrogen passivation at 450 °C for 2 h. The final cell area after edge isolation was 144 cm^2 for Polix and 119 cm^2 for Baysix.

5.1 Illuminated IV-measurements

The parameters of the illuminated IV-measurements are given in Table II for the best Baysix and Polix cells in this experiment.

Table II: Illuminated IV-parameters of mechanically V-textured solar cells on Polix (144 cm^2) and Baysix (119 cm^2). The cells are coated with a single layer ARC of LPCVD SiN_x. The result of Polix was indepently confirmed at FhG-ISE callab, Germany.

	V_{oc} [mV]	J_{sc} [mA/cm^2]	FF [%]	η [%]
Polix	628	36.3	76.8	17.5
Baysix	603	36.0	76.1	16.5

The efficiency of 17.5% on Polix was independently confirmed at FhG-ISE callab, Germany. The illuminated IV-characteristics as measured at FhG-ISE under standard test conditions (AM 1.5, 1000 W/m^2, T=25 °C) are shown in Figure 4. An efficiency of 17.5% is, to the best knowledge of the authors, the highest efficiency obtained on a solar cell area equal or larger than 100 cm^2 on mc-Si. A very high V_{oc} of 628 mV and J_{sc} of 36.3 mA/cm^2 were measured, which are amongst the highest values obtained for large area mc-Si solar cells. The front surface is only coated with a single layer ARC of SiN_x, allowing a further increase in J_{sc} by the deposition of a second layer ARC. The fill factor of 76.9% is rather moderate and will be discussed in more detail in the next section. Also a good efficiency of 16.5% was attained on Baysix. A similar J_{sc} of
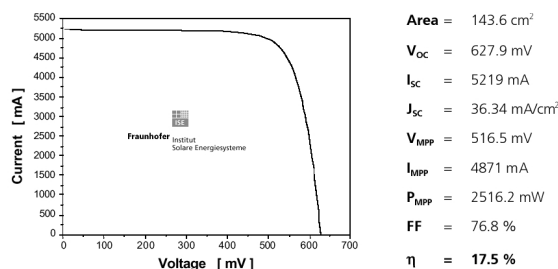

Figure 4: Illuminated IV-characteristics of Polix as measured at FhG-ISE callab.

36 mA/cm^2, but a reduced V_{oc} of 603 mV was obtained mainly due to a lower base doping level of the Baysix material.

5.2 Dark IV and J_{sc}-V_{oc} characteristics

For further solar cell characterisation, the parameters of the Two-Diode model were determined from a fit to the dark IV-, illuminated IV- and J_{sc}-V_{oc} characteristics. The J_{sc}-V_{oc} curve was obtained by measuring V_{oc} and J_{sc} at different light intensities using a flash light.
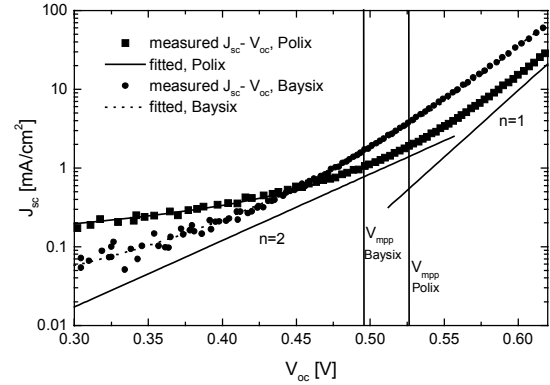

Figure 5: Measured and fitted J_{sc}-V_{oc} characteristics for Polix and Baysix. The vertical lines illustrate the voltage at maximum power point for Polix and Baysix, respectively.

The shunt resistance was fitted in the negative range of the dark IV-characteristics. J_{01} and J_{02} were determined from the J_{sc}-V_{oc} curve and the series resistance from the illuminated IV-characteristics. For the ideality factors, n_1=1 was taken for the first diode and n_2=2 for the second diode.

Table III: Diode parameters determined from a fit of the Two-Diode model to the dark, illuminated and J_{sc}-V_{oc} characteristics.

Mc-Si	J_{01} [pA/cm^2]	J_{02} [nA/cm^2]	R_{sh} [Ωcm^2]	R_s [Ωcm^2]
Polix	0.76	36	1600	0.62
Baysix	1.9	66	8000	0.62

The measured and fitted J_{sc}-V_{oc} curves are shown in Figure 5, the parameters of the Two-Diode model are given in Table III. The series resistance, R_s, is about 0.6 Ωcm^2, which is a reasonably low value for a large area solar cell indicating the high quality front side metallisation. Hence, the series resistance is not responsible for the relatively moderate fill factor.

For Baysix, the saturation current density of the second diode, J_{02}, was determined to be 6.6×10^{-8} A/cm^2. At the maximum power point, the slope deviates from its ideal value of n=1 and therefore indicates the influence of J_{02}. A reduction to J_{02}=1×10^{-8} A/cm^2 will increase V_{oc} by ΔV_{oc}=5.4 mV (0.9%rel.) and the fill factor by ΔFF=2.6%abs. (3.3%rel.). Hence the rather moderate fill factor can be explained by a high J_{02}. Different reasons are possible for the increase in current at low voltages leading to the deviations from n=1. First of all, it could be caused by SRH-recombination in the space charge

region due to crystal defects or metallic impurities. A high value of J_{02} would then be inherent to mc-Si and a reduction could, in principle, be achieved by the elimination or passivation of these defects in the space charge region. Additionally, the high J_{02} could be caused by the solar cell design, the process technology or the solar cell metallisation. However, BCSCs on Cz-Si manufactured with a similar processing sequence lead to J_{02} of about $1-2 \times 10^{-8} A/cm^2$. This strongly suggests that the high J_{02} is due to intrinsic material properties of the mc-Si material.

For Baysix, a shunt resistance R_{sh} of 8000 Ωcm^2 was determined which will not negatively influence the fill factor and therefore efficiency. For Polix, R_{sh} determined at negative voltages was 2900 Ωcm^2. However, under forward bias, an increase in the current is observed for lower voltages, which can be described by decreasing R_{sh} to about 1600 Ωcm^2. Hence, the moderate fill factor of Polix can be explained by a low R_{sh} and relatively high J_{02}, which is most probably also caused by intrinsic material properties of the mc-Si material.

5.3 Spectral analysis

Spectral response and reflectivity measurements were done to determine the Internal Quantum Efficiency (IQE) and External Quantum Efficiency (EQE). The IQE, EQE and reflectivity of Polix is given in Figure 6. The very low reflectivity demonstrates the high quality of mechanical V-texturing applying the single blade approach. The high IQE in the red wavelength region indicates a high effective diffusion length, L_{eff}.

Local LBIC and reflectivity measurements were carried out on Polix and are given as mapping of the IQE at λ=980 nm in Figure 7. The mapping shows an excellent homogeneity of the Polix material with only a small number of grains with a low IQE. However, these grains could lead to the "shunting" behaviour discussed in the previous section.

5.4 Loss analysis

In this section, a loss analysis is carried out for the Polix solar cell. In general, the losses can be divided into optical, resistive and recombination losses. The recombination losses can be further divided into losses of
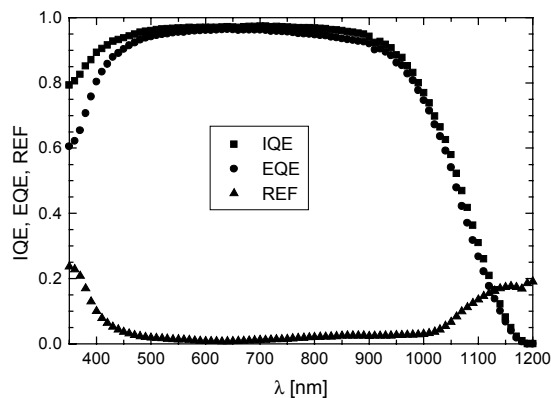

Figure 6: Internal Quantum Efficiency (IQE), External Quantum Efficiency (EQE) and reflectivity (REF) for mechanically V-textured BCSCs on Polix mc-Si.
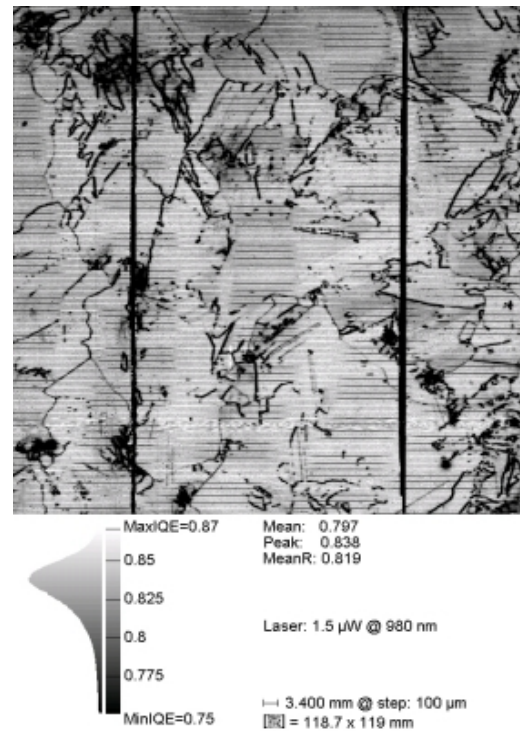

Figure 7: Mapping of the Internal Quantum Efficiency IQE of Polix mc-Si solar cell at λ=980 nm obtained from local LBIC and reflectivity measurements.

the emitter and of the base. The determination of the optical and recombination losses are based on an evaluation of the IQE using an electrical and optical model similar to the one used in IQE1D [13] extended by free carrier absorption.

The basic feature of the cell are low shadowing losses and a moderate rear surface reflectivity, R_b, of about 70%. The metal coverage on the front is 4.0% (finger width of 28 μm, finger spacing 1.4 mm and busbar width of 1 mm). Based on the device design with a mechanically V-textured solar cell, a single layer ARC and the above mentioned shadowing losses, the current density actively absorbed in the cell is about 39.5 mA/cm^2. Incomplete carrier collection causes the difference of 3.2 mA/cm^2 between the measured J_{sc} and the absorbed current of which 0.7 mA/cm^2 is lost by recombination in the emitter. The rather high emitter losses are caused by an unintended low emitter sheet resistance of 70-80 Ω/sqr. Generally, we obtain emitter losses for BCSCs of about 0.2-0.3 mA/cm^2 with an optimised emitter as well as front surface passivation. The IQE spectrum appeared not to contain sufficient information to reliably separate the remaining 2.5 mA/cm^2 into rear and bulk recombination.

The effective diffusion length of 340 μm gives a contribution to J_{01} of approx. 230 fA/cm^2 on the 0.5 Ωcm material. The emitter contribution, J_{oe}, therefore dominates already over the base and rear (about 300 fA/cm^2 as determined on test samples, including the surface enlargement by V-texturing).

5.5 Potential for efficiency improvements

Based on the solar cell parameters of Polix and on the results of the loss analysis, the potential for a higher solar cell efficiency is discussed for the applied BCSC process of this work. An increase in solar cell efficiency can be accomplished by the reduction of the emitter losses. If the emitter losses are reduced by 0.5 mA/cm^2 an efficiency of 17.8% can be achieved. A further increase can be attained by an increase in the shunt resistance R_{sh} to 10 kΩcm^2 and a decrease in the series resistance to 0.45 Ωcm^2, which we have already achieved for other large area BCSCs. Hence an efficiency of 18% seems possible on large area BCSCs on mc-Si with the same material quality.

Table IV: Possibilities for a further increase in solar cell efficiency based on the results obtained on Polix.

	V_{oc} [mV]	J_{sc} [mA/cm^2]	FF [%]	η [%]
Polix	628	36.3	76.8	17.5
Reduction in emitter losses	628.5	36.8	76.8	17.8
R_{sh}=10 kΩcm^2	628.8	36.8	77.5	17.9
R_s=0.45 Ωcm^2	628.8	36.8	77.8	18.0

Further increases can be expected by the application of improved light trapping, which requires a modification of the processing sequence. For example, a gain in J_{sc} of about 0.5 mA/cm² can be achieved by increasing the rear surface reflectivity, R_b, to 90% by application of a back surface reflector.

6 CONCLUSION

In this paper, a record high efficiency of a large area multicrystalline silicon solar cell of 17.5% has been presented with a high open circuit voltage of 628 mV and a short circuit current density of 36.3 mA/cm^2. Mechanical V-texturing using single blades leads to low front surface reflection losses comparable to alkaline texturing on Cz-Si. Remote hydrogen passivation increased the efficiency by 1.0%abs. on Baysix and by 0.4%abs. on Eurosil. The record high efficiency follows from a good final bulk diffusion length exceeding the cell thickness, from very low optical losses due to low grid shadowing losses and due to low front surface reflectivity. The buried contact solar cell design with metallisation by electroless plating leads to low shadowing losses and low resistive losses with R_s of about 0.6 Ωcm^2. Intrinsic properties of the mc-Si material leading to a high J_{02} and/or low R_{sh} are responsible for a relatively moderate fill factor below 77%.

7 ACKNOWLEDGMENTS

8 REFERENCES

[1] J. Zhao, A. Wang, M. A. Green, "19.8 % efficient 'honeycomb' textured multicrystalline and 24.4 % monocrystalline silicon solar cells", Appl.Phys.Lett., **73** (14), pp.1991-1993

[2] Y. Komatsu, Y. Takaba, S. Yasukawa, S. Okamoto, M. Shimizu, "Front-side surfce recombination analysis of 18%-efficient multicrystalline silicon solar cell", Proc. 12th Workshop on Crystalline Silicon Solar Cell Materials and Processes 2002, pp. 87-94

[3] H. Nakaya, M. Nishida, Y. Takeda, S. Moriuchi, T. Tonegawa, T. Machida, T. Nunoi, "Polycrystalline silicon solar cells with V-grooved surface", Sol. En. Mat. and Solar Cells **34** (1994), pp. 219-225

[4] K. Fukui, K. Okada, Y. Inomata, H. Takahashi, S. Fujuii, Y. Fukawa, K. Shirasawa, "Surface and bulk-passivated large area multicrystalline silicon solar cells", Sol. En. Mat. and Solar Cells **48** (1997), pp. 219-228

[5] W. Jooss, P. Fath, E. Bucher, S. Roberts, T. M. Bruton, "Large area multicrystalline silicon buried contact solar cells with bulk passivation and an efficiency of 17.5%", to be published in Proc. 29th IEEE PVSC New Orleans 2002

[6] S. R. Wenham, M. A. Green, US Patent No. 4,726,850 (1988)

[7] T. M. Bruton, Sol. En Mat. and Solar Cells **72** (2002), pp. 3-10

[8] W. Jooss, P. Fath, E. Bucher, S. Roberts, T. M. Bruton, "Process Development for Large Area Buried Contact Solar Cells on Multicrystalline Silicon", Proc. 17th EC PVSEC Munich 2001

[9] C. Gerhards, A. Fischer, M. Spiegel, P. Fath, E. Bucher, B. Leifhelm, M. Weck, "High throughput mechanical structuring system for solar cell wafers", Proc. 17th EC PVSEC Munich 2001

[10] Ch. Zechner, "Mechanisch texturierte Solarzellen und Rückkontaktsolarzellen aus kristallinem Silizium", PhD thesis, University of Konstanz, 1999

[11] R. Kühn, P. Fath, M. Spiegel, G. Willeke, E. Bucher, T. M. Bruton, N. B. Mason, R. Russell, "Multicrystalline buried contact solar cells using a new electroless plating metallisation sequence and a high throughput mechanical groove formation", Proc. 14th EC PVSEC Barcelona 1997, pp. 672-677

[12] M. Spiegel, S. Keller, P. Fath, G. Willeke, E. Bucher, "Microwave induced remote hydrogen plasma (MIRHP) passivation of solar cells using different silicon base materials", Proc. 14th ECPVSEC Barcelona 1997, pp. 743-746

[13] R. Brendel, R. Plieninger, "IQE1D, Program for the analysis of solar cell quantum efficiency measurements", Vertrieb Garching Innovation GmbH München 1996